The Aeronautical Journal (2024), **128**, pp. 2656–2667
doi:10.1017/aer.2024.44

RESEARCH ARTICLE

Maximisation the autonomous flight performance of unmanned helicopter using BSO algorithm

M. Konar and S. Arık Hatipoğlu

Department of Aircraft Electrical and Electronics, Faculty of Aeronautics and Astronautics, Erciyes University, Kayseri, Türkiye
Corresponding author: M. Konar; Email: mkonar@erciyes.edu.tr

Received: 9 November 2023; **Revised:** 11 March 2024; **Accepted:** 3 April 2024

Keywords: back-tracking search optimisation; autonomous flight performance; helicopters; UAV; optimisation

Abstract

The usage areas of rotary or fixed wing unmanned aerial vehicles (UAV) have become very widespread with technological developments. For this reason, UAV designs differ in terms of aerodynamic design, flight performance and endurance depending on the intended use. In this study, maximising of the autonomous flight performance of the unmanned helicopter produced at Erciyes University using an optimisation algorithm is discussed. For this purpose, the input parameters of the dynamic model are chosen as blade length, blade mass density, blade chord width and blade twist angle of the unmanned helicopter and the proportional, integral, derivative gain coefficients of the lateral axis of the autopilot. The output parameters of the dynamic model are selected as settling time, rise time and maximum overshoot, which are autonomous performance parameters. The dynamic model consisting of helicopter and autopilot parameters is integrated into the back-tracking search optimisation (BSO) algorithm as an objective function. In the optimization process, where mean squared error (MSE) is used as the performance criterion, optimum input and output values were determined. Thus, helicopter and autopilot parameters, which are among the factors affecting autonomous performance, are taken into account with equal importance and simultaneously. Simulations show that the obtained values are satisfactory. With this approach based on the optimisation method, complex and time-consuming dynamic model calculations are reduced, time and cost are saved, and practicality is achieved in applications. Therefore, this approach can be an innovative and alternative method to improve UAV designs and increase flight performance compared to classical methods.

Nomenclature

UAV:	unmanned air vehicle
BSO:	back-tracking search optimisation
MSE:	mean squared error
ANN:	artificial neural network

1.0 Introduction

With their technological capabilities, unmanned aerial vehicles (UAVs) meet the requirements of both military and civilian applications. Many fields such as robotics, electronic hardware and software contribute to UAV technologies [1–6].

Today, UAVs can perform their tasks as semi-autonomous or fully autonomous, with UAV systems with simple or advanced security protocols. The sizes of UAVs designed for different tasks also differ. Fixed and rotary wing types of UAVs in mini size are widely produced. However, in large size, fixed-wing types are generally produced more widely due to the difficulties of application and use.

© The Author(s), 2024. Published by Cambridge University Press on behalf of Royal Aeronautical Society.

https://doi.org/10.1017/aer.2024.44 Published online by Cambridge University Press

In the production of UAVs or helicopters, designs that concern sub-disciplines such as aerodynamics, structure-strength and materials science are carried out. Then, expert production engineers and technicians produce the UAV or helicopter, whose sub-designs are completed. After manufacturing, the autopilot phase is carried out by expert control engineers using the technical data of the produced UAV or helicopter. At this phase, either a new autopilot is manufactured, or the parameters of an existing autopilot are adjusted. These work packages often require simultaneous consideration of design and manufacturing activities and control system activities to achieve optimal flight performance.

The use of optimisation methods makes a great contribution to different problem solutions involving parameters that need to be handled simultaneously. By using many different heuristic algorithms, parameters with minimum and maximum values can be estimated optimally under certain conditions. The use of heuristic algorithms in many studies such as aerodynamic design, thrust system design, increasing endurance and range, and autonomous system design offers a good alternative to designers in obtaining the best-desired solution [1–4, 6].

In the literature, there are many studies about rotary wing air vehicles [7–12]. In one of the studies presented, some structural parameters of the helicopter were revised and the performance was tried to be improved [9, 10]. In another study, rotor dynamics and flight dynamics were simultaneously optimised using some design parameters [7]. In another study, vibration loads on the rotor hub, which is the main source of helicopter vibration, were reduced by using the main variables such as the torsional stiffness of the helicopter blade [8]. In another study, some parameters of the helicopter and the output variance were simultaneously examined using a constrained controller, and the redesign of the helicopter to minimise the control energy was discussed [12]. In another study, it was tried to obtain the optimum thrust-torque ratio by changing the blade parameters [4]. In another study, a model based on back-tracking search optimisation (BSO)-based artificial neural network (ANN) has been proposed to maximise the performance and flight time of the UAV's brushless motor [13].

In this study, it is aimed to maximise the autonomous flight performance of the unmanned helicopter produced in Erciyes University Faculty of Aeronautics and Astronautics by using innovative methods. A dynamic model of this unmanned helicopter having some features, such as medium range, medium altitude, medium endurance and electrically driven, has been produced. However, there are many parameters that affect autonomous flight performance. In this study, helicopter blade parameters and autopilot parameters, which significantly affect autonomous flight performance, are determined as inputs, and autonomous performance parameters are determined as outputs. The blade length (b), blade mass density (m), blade chord width (c) and blade twist angle (t) of the unmanned helicopter and the proportional (P), integral (I), derivative (D) gain coefficients of the lateral axis of the autopilot are selected as input parameters of the dynamic model. Settling time (s), rise time (r) and maximum overshoot (o), which are autonomous performance parameters, are determined as output parameters of the dynamic model. This dynamic model with complex relations is determined as a cost function of the algorithm and integrated into the BSO algorithm. However, in order to obtain reasonable results during the optimisation process, certain limit values have been applied for helicopter blade parameters and autopilot parameters. These limits are set so that the helicopter blade parameters do not change more than $\pm 5\%$ from the nominal values and the autopilot gain coefficients do not change more than $\pm 25\%$ from the recommended values. Thus, the gain parameters of the autopilot system were calculated to minimise the autonomous performance index together with helicopter variables simultaneously. In other words, optimum input values are calculated by considering the autonomous performance parameters simultaneously and at equal importance with the BSO algorithm.

With this study, the simultaneous optimisation of the electric unmanned helicopter rotor system and the flight control system has been realised together for the first time in the literature. Thus, it is ensured that design and manufacturing activities and control system activities are handled simultaneously in order to achieve maximum flight performance. In addition, the BSO algorithm was used for the first time in the literature for this purpose, and the results emphasised that heuristic methods can be used as an alternative method in the literature.

https://doi.org/10.1017/aer.2024.44 Published online by Cambridge University Press



Figure 1. *Photo of the manufactured helicopter.*

2.0 Dynamic model of our unmanned helicopter

Helicopters include one or more rotors and two or more rotor blades. Helicopters can fly via this rotor and blades. The helicopters do not require forward acceleration like airplanes thanks to their vertical take-off and landing capabilities. While the source of lift in aircraft is wings, the source of lift in helicopters is rotor blades rotating around a mast. This gives helicopters the ability to take-off and land vertically without the need for a runway. For this reason, helicopters can generally be used in areas where fixed-wing aircraft cannot land. Besides being able to take-off and land vertically, they are used to perform tasks that require time or work intensity thanks to their ability to hover for a long time [14–17].

The power required in helicopters is produced by the rotor. A helicopter rotor consists of mast, hub and rotor blades. The mast is a hollow cylindrical metal shaft extending upwards and driven by the transmission. At the top of the mast is the connection point of the rotor blades, called the hub. The rotor blades are attached to this hub in a number of different ways and constitute the necessary lift. For this reason, it is very important to select the blades with optimum features.

In this section, dynamic model and some properties of our unmanned helicopter are explained briefly.

2.1 Dynamic model and some properties of our unmanned helicopter

To capture the main physics and essential dynamics, we derived the dynamic model of the unmanned helicopter from a finite set of ordinary differential equations. The model of our helicopter, whose photo is given in Fig. 1, has a rather complex structure as it includes the fuselage, fully articulated (i.e. with four blades) main rotor, tail rotor, landing gear, empennage and main rotor downwash. There are 29 dynamic equations in the model, including 9 fuselage, 3 static main rotor downwash, 16 blade flapping and lead-lagging and an additional flight path angle algebraic equation [7–10].

During the obtaining of the dynamic model of the helicopter, many sources related to the helicopters were utilised [14–16, 18–27]. At first, Newton's second law and the law of conservation of angular momentum (Euler's law) were used in order to obtain the force and moment equations of the helicopter, respectively. The dimensionless force and moment equations are given in Equations (1) and (2), respectively. The process of non-dimensioned is widely used in studies on helicopters for ease of calculation. Here, X, Y, Z are the longitudinal, lateral and vertical forces in the x- y- and z- directions in the airplane axis set, respectively. L, M, N are the rolling, pitching and yawing moments in the

https://doi.org/10.1017/aer.2024.44 Published online by Cambridge University Press

x- *y*- and *z*- directions, respectively. All sub-components of the helicopter contribute to these forces and moments.

$$\begin{aligned}
&\frac{d}{d\psi}\hat{u}+\hat{q}\hat{w}-\hat{r}\hat{v}+\frac{g\sin(\theta_A)}{\Omega^2 R}=\frac{X}{\Omega^2 R M_a}\\
&\frac{d}{d\psi}\hat{v}+\hat{r}\hat{u}-\hat{p}\hat{w}-\frac{g\cos(\theta_A)\sin(\phi_A)}{\Omega^2 R}=\frac{Y}{\Omega^2 R M_a}\\
&\frac{d}{d\psi}\hat{w}+\hat{p}\hat{v}-\hat{q}\hat{u}-\frac{g\cos(\theta_A)\cos(\phi_A)}{\Omega^2 R}=\frac{Z}{\Omega^2 R M_a}
\end{aligned} \tag{1}$$

$$\begin{aligned}
&\frac{d}{d\psi}\hat{p}-\hat{q}\hat{r}\left(\frac{I_{yy}}{I_{xx}}-\frac{I_{zz}}{I_{xx}}\right)-\frac{I_{xz}}{I_{xx}}\left(\hat{p}\hat{q}+\frac{d}{d\psi}\hat{r}\right)=\frac{L}{I_{xx}\Omega^2}\\
&\frac{d}{d\psi}\hat{q}-\hat{p}\hat{r}\left(\frac{I_{zz}}{I_{yy}}-\frac{I_{xx}}{I_{yy}}\right)+\frac{I_{xz}}{I_{yy}}\left(\hat{p}^2-\hat{q}^2\right)=\frac{M}{I_{yy}\Omega^2}\\
&\frac{d}{d\psi}\hat{r}-\hat{p}\hat{q}\left(\frac{I_{xx}}{I_{zz}}-\frac{I_{yy}}{I_{zz}}\right)-\frac{I_{xz}}{I_{zz}}\left(\hat{q}\hat{r}-\frac{d}{d\psi}\hat{p}\right)=\frac{N}{I_{zz}\Omega^2}
\end{aligned} \tag{2}$$

Sub-components such as main rotor, fuselage, empennage and landing gear play the most effective role in helicopter dynamics. Equation (3) refers to the kinematic equations of the helicopter. In Equation (4), the expression of the infinitesimal aerodynamic force acting on a blade at an x dimensionless distance from the blade root of any of the blades connected to the helicopter main rotor is presented. By integrating this expression along the blade root, the total aerodynamic force acting on that blade can be found. The sub-index F seen in this equation indicates that the force is obtained on the axis of flapping. The blades of the unmanned helicopter are produced with 2 degrees of freedom as feathering and fluttering. In this study, the forward-reverse movement is neglected as it has little contribution to helicopter dynamics. The moment affecting the infinite small blade element is given in Equation (5). Similarly, this moment expression is integrated along the blade to obtain the total aerodynamic moment acting on the blade.

$$\begin{aligned}
&\hat{p}=\frac{d}{d\psi}\phi_A-\frac{d}{d\psi}\psi_A\sin(\theta_A)\\
&\hat{q}=\frac{d}{d\psi}\psi_A\cos(\theta_A)\sin(\phi_A)+\frac{d}{d\psi}\theta_A\cos(\phi_A)\\
&\hat{r}=\frac{d}{d\psi}\psi_A\cos(\theta_A)\cos(\phi_A)-\frac{d}{d\psi}\theta_A\sin(\phi_A)
\end{aligned} \tag{3}$$

$$d_F F_{aero}=\frac{\gamma I_b}{2R^3}\begin{bmatrix}0\\ -\left(\theta U_T^2-U_P U_T\right)\dfrac{U_P}{U_T}-\dfrac{1}{a_0}\left(\delta_0+\delta_2\left(\theta-\dfrac{U_P}{U_T}\right)^2\right)\\ \theta U_T^2-U_P U_T\end{bmatrix}dx \tag{4}$$

$$d_F M_{aero}=\begin{bmatrix}0 & -xR(d_F F_{aero})_{III} & xR(d_F F_{aero})_{II}\end{bmatrix}^T \tag{5}$$

In Equations (6) and (7), a state-space model is presented for cruising flight with a specific speed of 10km/h. Using the numerical values given in Equations (6) and (7), the state-space model to be used in the simulation of the helicopter can be created. The state-space model is in the form of $\dot{x}=Ax+Bu$, $xy=Cx+Du$. Using the A matrix, the flight dynamics modes of our nominal unmanned helicopter are

https://doi.org/10.1017/aer.2024.44 Published online by Cambridge University Press

obtained [26]. Also, state variables and control elements are presented in Equations (8) and (9).

$$A_{10}=\begin{bmatrix}
-3.7571e\text{-}3 & -4.5367e\text{-}4 & -2.5697e\text{-}4 & -2.4461e\text{-}3 & -8.7688e\text{-}4 & 3.2019e\text{-}5 & 0 & -5.1688e\text{-}4 & 0 & 2.9857e\text{-}5 & 2.2572e\text{-}6 & -7.1653e\text{-}2 & -6.4565e\text{-}4 & -6.4481e\text{-}4 & 1.0518e\text{-}4\\
5.0593e\text{-}4 & -2.4107e\text{-}3 & 5.0678e\text{-}5 & 9.9473e\text{-}4 & -2.6639e\text{-}3 & -2.2717e\text{-}2 & 5.1638e\text{-}4 & -7.2025e\text{-}7 & 0 & 2.6344e\text{-}6 & 6.9718e\text{-}5 & -7.2925e\text{-}4 & 5.0157e\text{-}5 & 8.0935e\text{-}2 & 7.3005e\text{-}4\\
6.9742e\text{-}5 & 5.2214e\text{-}6 & -6.2141e\text{-}3 & -9.0886e\text{-}5 & 2.2885e\text{-}2 & 1.8526e\text{-}8 & 2.2926e\text{-}5 & 1.6222e\text{-}5 & 0 & -1.0353e\text{-}1 & -2.2797e\text{-}3 & 7.0122e\text{-}5 & 4.7094e\text{-}8 & 1.0130e\text{-}5 & 1.2243e\text{-}7\\
-2.3661e\text{-}2 & 6.4710e\text{-}2 & -3.1532e\text{-}3 & -5.7314e\text{-}2 & 8.8674e\text{-}2 & -6.9175e\text{-}3 & 0 & 0 & 0 & 1.1332e\text{-}3 & -2.9127e\text{-}3 & 3.4232e\text{-}2 & 2.2289e\text{-}2 & -3.7745 & -3.4245e\text{-}2\\
-1.1152e\text{-}1 & -2.1140e\text{-}2 & -1.3231e\text{-}2 & -7.8454e\text{-}2 & -5.2497e\text{-}2 & -1.1927e\text{-}10 & 0 & 0 & 0 & 2.4985e\text{-}3 & -1.8535e\text{-}4 & -3.3409 & -3.0305e\text{-}2 & -3.0258e\text{-}2 & -1.9747e\text{-}2\\
-2.0369e\text{-}3 & 9.2391e\text{-}2 & 3.1551e\text{-}1 & -4.4414e\text{-}2 & 9.2267e\text{-}3 & -1.8715e\text{-}2 & 0 & 0 & 0 & 7.0729e\text{-}5 & -1.8535e\text{-}1 & -5.9529e\text{-}4 & 2.5422e\text{-}3 & -5.0443e\text{-}1 & -4.0437e\text{-}3\\
0 & 0 & 0 & 1 & 1.3934e\text{-}3 & -3.1385e\text{-}2 & 0 & 0 & 0 & 0 & 0 & 0 & 0 & 0 & 0\\
0 & 0 & 0 & 0 & 9.9902e\text{-}1 & 4.4355e\text{-}2 & 0 & 0 & 0 & 0 & 0 & 0 & 0 & 0 & 0\\
0 & 0 & 0 & 0 & -4.4377e\text{-}2 & 9.9951e\text{-}1 & 0 & 0 & 0 & 0 & 0 & 0 & 0 & 0 & 0\\
0 & 0 & 0 & 0 & 0 & 0 & 0 & 0 & 0 & 0 & 1 & 0 & 0 & 0 & 0\\
-7.0425e\text{-}4 & -1.7752e\text{-}3 & 2.0293 & 2.2742e\text{-}2 & 2.7555e\text{-}4 & 7.3075e\text{-}7 & 0 & 0 & 0 & -4.0838 & -1.1317 & -6.8539e\text{-}3 & -2.1490e\text{-}5 & 4.1207e\text{-}4 & -1.6096e\text{-}2\\
0 & 0 & 0 & 0 & 0 & 0 & 0 & 0 & 0 & 0 & 0 & 1 & 0 & 0 & 0\\
-1.6723e\text{-}1 & 1.0373e\text{-}1 & -1.9094e\text{-}2 & 2.8262 & 1.5241 & -1.7292e\text{-}10 & 0 & 0 & 0 & -4.3009e\text{-}2 & -6.5480e\text{-}4 & -7.9274 & -1.1756 & -1.1759 & -2.0286\\
0 & 0 & 0 & 0 & 0 & 0 & 0 & 0 & 0 & 0 & 0 & 0 & 0 & 0 & 1\\
9.9925e\text{-}2 & 9.9317e\text{-}2 & 5.8161e\text{-}2 & 1.5171 & -2.8113 & -1.0029e\text{-}2 & 0 & 0 & 0 & 1.7079e\text{-}3 & -3.6425e\text{-}2 & 1.1809 & 2.0323 & -8.5560 & -1.1813
\end{bmatrix} \tag{6}$$

$$B_{10}=\begin{bmatrix}
-7.5251e\text{-}6 & 2.9914e\text{-}4 & -1.8460e\text{-}4 & 5.8177e\text{-}13\\
-4.2867e\text{-}5 & -8.8132e\text{-}5 & -3.3865e\text{-}4 & 2.6913e\text{-}4\\
1.0532e\text{-}3 & -1.0382e\text{-}7 & -1.2207e\text{-}4 & 1.6965e\text{-}8\\
2.0993e\text{-}3 & -3.9155e\text{-}2 & 1.5894e\text{-}2 & -6.3348e\text{-}3\\
1.3902e\text{-}3 & 1.4041e\text{-}2 & 3.4658e\text{-}2 & -1.0922e\text{-}10\\
3.2517e\text{-}1 & -4.4095e\text{-}3 & 8.2065e\text{-}3 & -1.2337e\text{-}1\\
0 & 0 & 0 & 0\\
0 & 0 & 0 & 0\\
0 & 0 & 0 & 0\\
0 & 0 & 0 & 0\\
1.5991 & 6.7585e\text{-}5 & 4.6626e\text{-}2 & 6.6919e\text{-}7\\
0 & 0 & 0 & 0\\
2.1455e\text{-}3 & 1.6191 & 5.0247e\text{-}2 & -1.5835e\text{-}10\\
0 & 0 & 0 & 0\\
9.6306e\text{-}2 & -5.6764e\text{-}2 & 1.6225 & -9.1840e\text{-}3
\end{bmatrix} \tag{7}$$

Here, the first three variables in the x vector are the velocity components in the three axes, the next three variables are the angular velocity components in the three axes, the next three variables are the orientation angles in the three axes, and the next three variables are the collective, longitudinal circular and laterally circular flapping angles and velocities, respectively. In addition, the vector u consists of collective, lateral and longitudinal circular main rotor pitch controllers and tail rotor control, respectively.

$$x=\begin{bmatrix}\hat{u} & \hat{v} & \hat{w} & \hat{p} & \hat{q} & \hat{r} & \phi_A & \theta_A & \psi_A & \beta_0 & \dot{\beta}_0 & \beta_c & \dot{\beta}_c & \beta_s & \dot{\beta}_s\end{bmatrix} \tag{8}$$

$$u=\begin{bmatrix}\theta_0 & \theta_c & \theta_s & \theta_T\end{bmatrix} \tag{9}$$

Some basic data of the unmanned helicopter used in the study are as follows: main rotor diameter is 1.5m, helicopter mass is 5kg, pitching moment of inertia is 3,849,417.1 $\times 10^{-9}$kg.m^2, yaw moment of inertia is 3,884,419.78 $\times 10^{-9}$kg.m^2, rolling moment of inertia is 93,550.65 $\times 10^{-9}$ kg.m^2.

In Equation (10), the trim vector used to obtain the numerical values of the state-space model for 10km/h is given. Here, respectively, the first two terms are the trim values of the pitch and roll angles of the whole helicopter in radians, the next three terms are the trim values in radians of the collective, longitudinal circular and laterally circular components of the flapping angles of the helicopter blades. The next three terms are the trim values in radians of the collective, longitudinal circular and laterally circular components of the pitch angles of main rotor, and the next one term is the trim value in radians of the pitch angle of tail rotor, respectively. The last three components are trim values in radians for terms related to main rotor down deflection.

$$_{10km/h}x_0=[\underbrace{\text{-4.4369e-2,-3.1406e-2}}_{\theta_{A_0},\phi_{A_0}},\underbrace{\text{2.7289e-3,-3.4427e-4,-3.3386e-4}}_{\beta_{0_0},\beta_{c_0},\beta_{s_0}},\underbrace{\text{1.3770e-1,-8.2354e-4,-2.3317e-3,1.6655e-1}}_{\theta_{0_0},\theta_{c_0},\theta_{s_0},\theta_{T_0}},\underbrace{\text{2.2692e-2,1.9861e-2,8.0780e-1}}_{\lambda_{0_0},\lambda_{c_0},\chi_0}] \tag{10}$$

https://doi.org/10.1017/aer.2024.44 Published online by Cambridge University Press

3.0 Problem definition and methods

In this section, simultaneous design, problem formulation and BSO algorithm are explained.

3.1 Problem definition

In this study, the changing of *b, m, c, t* of the electrically driven unmanned helicopter before the flight and the determining optimally of autopilot *P, I, D* gain coefficients were considered. In response to these helicopter variables selected as input, the autonomous performance parameters such as *s, r* and *o* were minimised. That is, a cost function with complex relations was obtained, where the helicopter variables are the input and the autonomous performance parameters are the output.

It is not analytically possible to take derivatives of this cost function, which has complex relations, according to the selected variables. For this reason, optimisation techniques are used to solve problems that have a complex relationship or cannot be directly related. In this study, the BSO algorithm is preferred to overcome this difficult problem that has complex relationship. These algorithmic methods have been used successfully in complex and constrained optimisation problems before. Thus, the gain parameters of the autopilot system were calculated simultaneously with the selected helicopter variables to minimise the autonomous performance index.

3.2 Problem formulation

The equation for the problem of determining autonomous performance parameters (settling time, rise time, maximum overshoot) by using helicopter parameters (blade length, blade mass density, blade chord width and blade twist angle) and autopilot system parameters (*P, I, D* gain coefficients) simultaneously is given in Equation (11).

$$opt_{helicopter\ param,\ control\ param} J = f_{\min\ (settling\ time,\ rise\ time,\ \max\ .overshoot)} \tag{11}$$

Here, *J* represents the jacobian matrix. In addition, there are certain limits on helicopter blade parameters and autopilot gain coefficients in the cost function expressed by Equation (1). The first of the limits is that the helicopter blade parameters cannot change more than the range of ±5 percentage of their nominal values determined by the manufacturer. The second of the limits is that the autopilot gain coefficients cannot change more than the range of ±25 percentage of the suggested value. The reason for these limits is that it allows making minor changes to the existing design to improve performance, rather than a design from scratch.

3.3 BSO algorithm

The BSO algorithm is a swarm-based evolutionary algorithm. The BSO algorithm provides global solutions by avoiding local solutions in optimisation problems. The study of the algorithm is based on five basic phases – initial values, first selection phase, mutation, crossing and second selection phase [28–30].

The initial value is defined by Equation (12). Here, *P* is the population size, *D* is the dimension of the problem. *Pi,j* represent a target individual in the population, and *lowj* and *upj* represent the lowest and highest limit values in the solution space, respectively.

$$P_{i,j} \sim U\left(low_j, up_j\right) \tag{12}$$

The first selection phase determines the *oldP* historical population to calculate the search direction. Thus, the BSO algorithm stores the values obtained in the past for use in the next decision-making mechanism. With the determination of *oldP*, population members are randomly reordered.

In the mutation (*M*) phase, the initial values of the mutant population are calculated by Equation (13). Here the *F* value adjusts the amplitude of the search matrix. Thus, the previous experiences are used to

https://doi.org/10.1017/aer.2024.44 Published online by Cambridge University Press

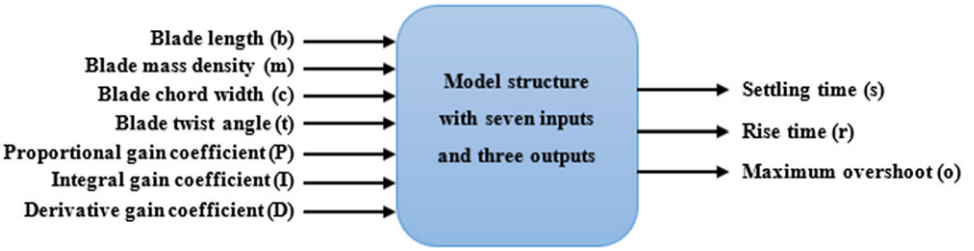


Figure 2. *Block diagram of the obtained model.*

determine the search direction.

$$M = P + F\,(oldP - P) \tag{13}$$

The crossing phase gives the final version of the population to be evaluated. Among the population members evaluated, those with good values according to the optimisation problem are used to identify the target population individuals. The BSO algorithm also uses the restriction mechanism to prevent mutated population individuals from exceeding their solution space limits.

The second selection phase is the phase where the update is done and the good one is selected. The global best value is checked again in each iteration by comparison with all population individuals. If any individual's cost function value is better than the current global best value, then the new global best value will be the position of this individual. The BSO algorithm can be easily applied to several engineering problems due to its very easy applicability [13, 28–30].

4.0 Simulation results

Determining the input and output parameters in optimisation methods is the first step. In this study, the data of the electric unmanned helicopter produced in Faculty of Aeronautics and Astronautics, Erciyes University was used. *b, m, c* and *t* of the electrical unmanned helicopter and the *P, I, D* gain coefficients of the autopilot were selected as input parameters. Autonomous performance parameters consisting of *s, r* and *o* were also selected as output parameters. Thus, a model with complex relations having seven inputs and three outputs was obtained. The block diagram of the obtained model is given in Fig. 2.

BSO algorithm was used to solve the cost function consisting of the model with complex relations. In the BSO algorithm, certain limits are applied to the input parameters and it is requested to obtain the minimum autonomous performance index from the algorithm. It has been adjusted so that the helicopter blade parameters (*b, c, m, t*) do not change more than ±5% from the nominal values, and the autopilot gain coefficients (*P, I, D*) do not change more than ±25% from the recommended values. The reference values of the input parameters used in the optimisation process are given as: *b* is 75cm, *m* is 0.2kg/m, c is 4.35cm, *t* is −0.14rad, *P* is 50, *I* is 5 and *D* is 50. Colony size and iteration, which are the control parameters of the BSO algorithm, were chosen as 50 and 500, respectively. To determine the optimisation performance realised with the BSO algorithm, MSE was chosen as the performance criterion.

As a result of BSO algorithm-based simulations, the input coefficients *b, c, m, t, P, I, D* were obtained as 1.026, 1.033, 0.950, 1.05, 0.796, 0.750, 1.25, respectively. In response to these input values, *s, r* and *o* that are autonomous performance parameters were calculated as 13.3151, 14.3859 and 1.2647, respectively.

In the BSO-based optimisation process, the changes of the coefficients of the input variables versus iteration are given in respectively from Fig. 3 to Fig. 9.

https://doi.org/10.1017/aer.2024.44 Published online by Cambridge University Press

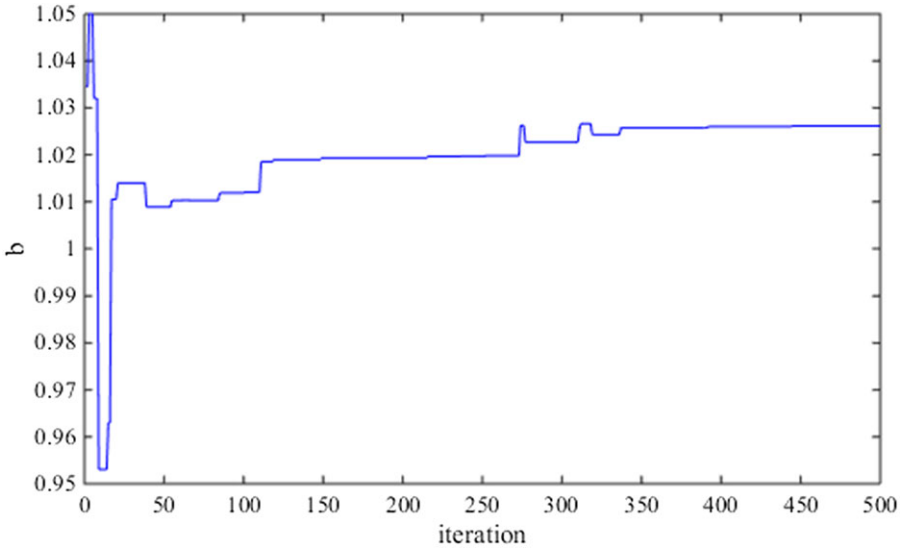


Figure 3. *The change graph of blade length coefficient versus iteration.*

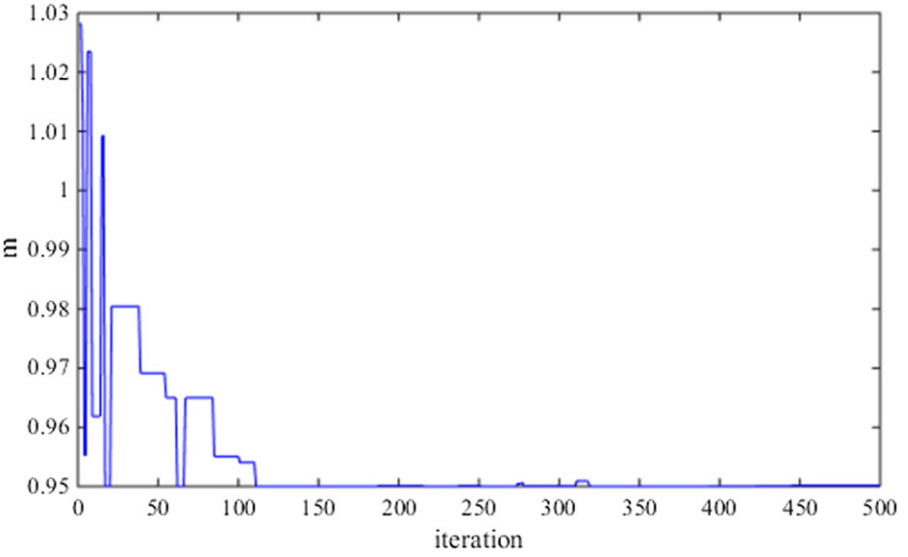


Figure 4. *The change graph of blade mass density coefficient versus iteration.*

When the results are examined, the coefficients of b, c and t tend to increase, while coefficient m tends to decrease. The fact that these results are satisfactory in terms of design improvement in practical application reveals the effectiveness of the method.

5.0 Conclusions

The development of technology has greatly influenced the development of fixed or rotary wing unmanned aerial vehicles and has encouraged the design of different sizes and types of aircraft for different missions.

https://doi.org/10.1017/aer.2024.44 Published online by Cambridge University Press

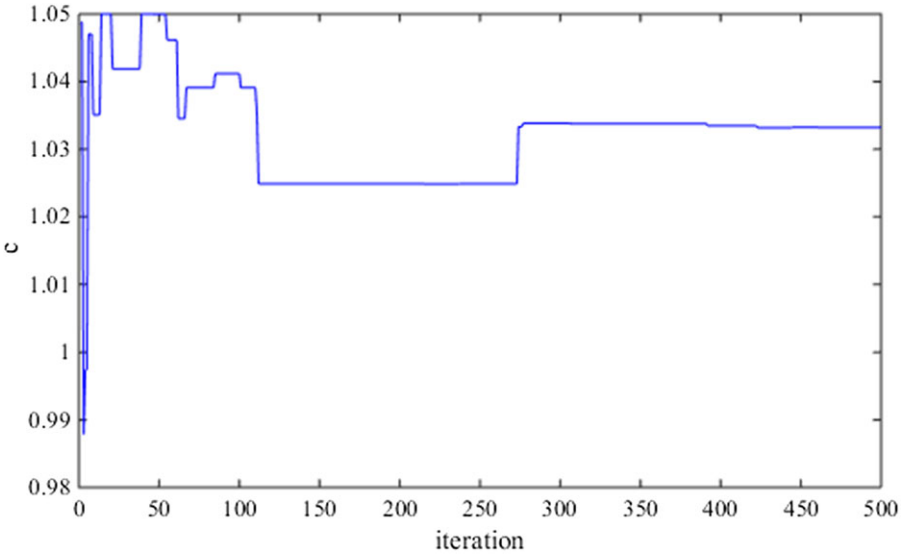


Figure 5. *The change graph of blade chord width coefficient versus iteration.*

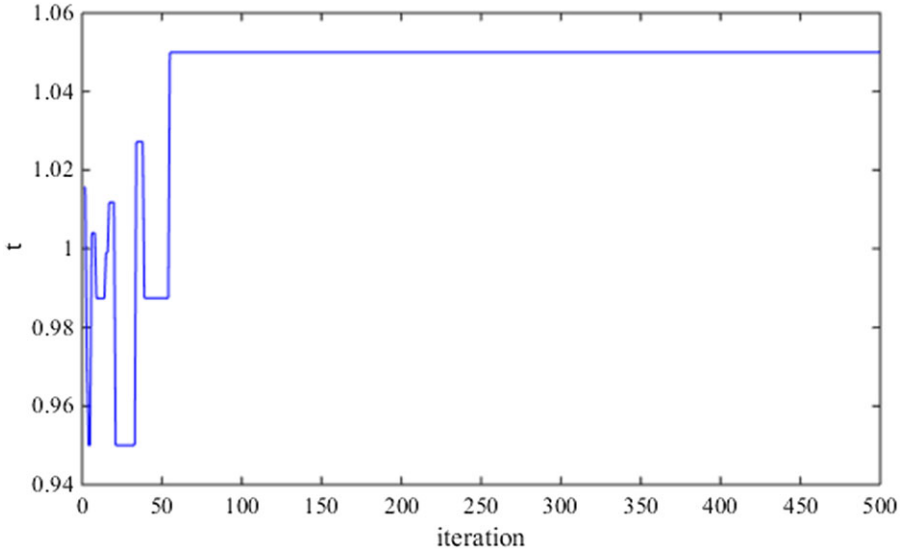


Figure 6. *The change graph of blade twist angle coefficient versus iteration.*

In this study, it is aimed to maximise the autonomous flight performance of the unmanned helicopter produced at Erciyes University. First, a dynamic model of this unmanned helicopter, which is electrically driven, was created. The reason for this is that there is no direct relationship between the input and output variables selected in the study. This dynamic model is used as a cost function in the BSO algorithm. In addition, simulations can be performed using wide limit values with optimisation algorithms. However, in this study, some limit values have been applied to the input values in order to obtain reasonable results in terms of practical applicability. New simulations can be performed by changing these limit values to various reasonable limit values in different studies. With the objective function created with the limit

https://doi.org/10.1017/aer.2024.44 Published online by Cambridge University Press

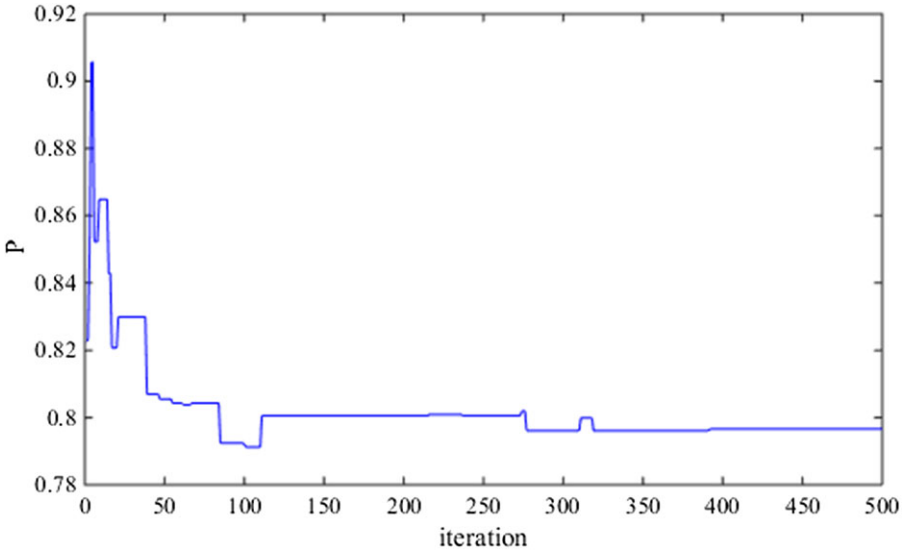


Figure 7. *The change graph of proportional gain coefficient versus iteration.*

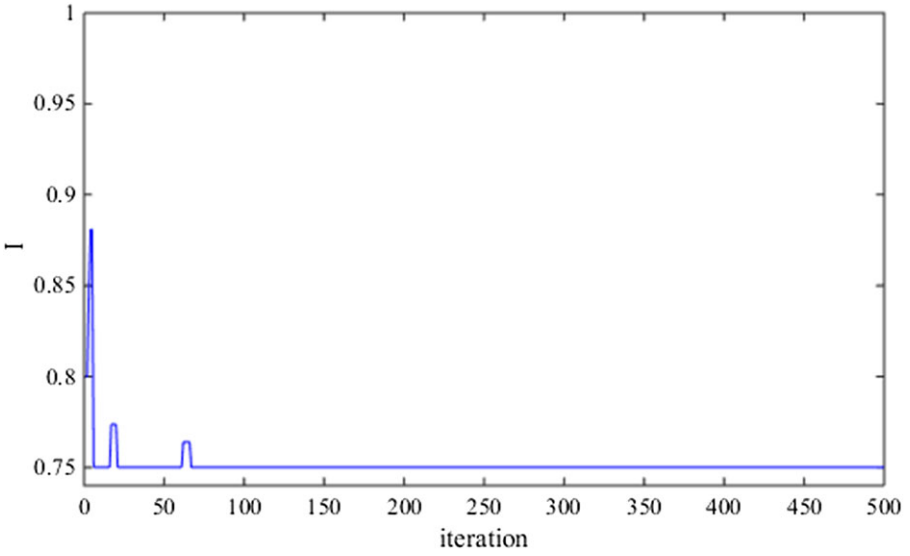


Figure 8. *The change graph of integral gain coefficient versus iteration.*

values determined in this study, the gain parameters of the autopilot system are calculated simultaneously with the helicopter variables to be of equal importance. The simulation results of our proposed model are presented in tables and figures. When the results are examined, it is seen that the obtained values are in the desired value ranges. This supports the success of the BSO algorithm in the optimisation process. The results also showed that the modeling provided an improvement of 29.92%. Therefore, it has been shown that this innovative method proposed in this study will be an alternative method for designers.

https://doi.org/10.1017/aer.2024.44 Published online by Cambridge University Press

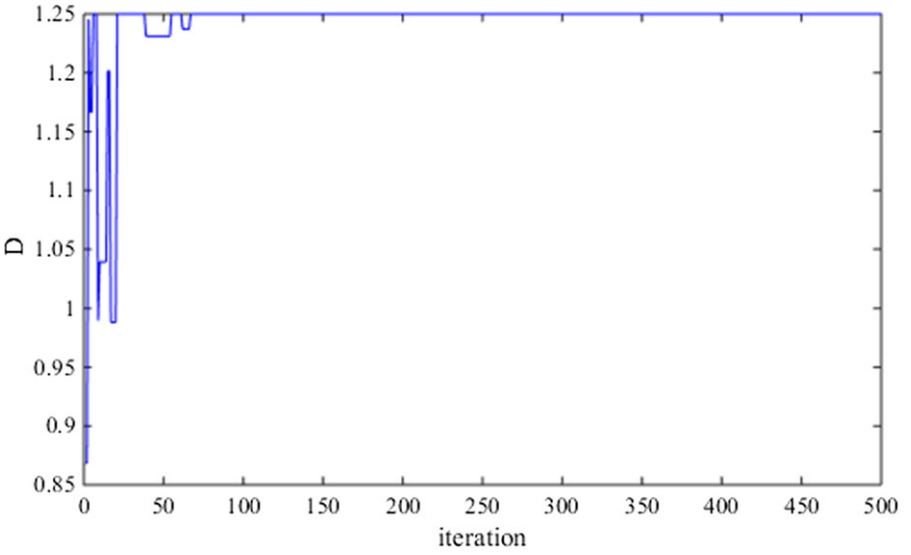


Figure 9. *The change graph of derivative gain coefficient versus iteration.*

Data availability statement. All data used during the study are available from the corresponding author by request.

Acknowledgment. This work was supported by Research Fund of Erciyes University Scientific Research Projects (BAP) Coordination Unit under Project Number: FBA-2018-7640.

References

[1] Arik, S., Turkmen, I. and Oktay, T. Redesign of morphing UAV for simultaneous improvement of directional stability and maximum lift/drag ratio, *Adv. Electr. Comput. Eng.*, 2018, **18,** (4), pp 57–62.
[2] Gur, O. and Rosen, A. Optimizing electric propulsion systems for unmanned aerial vehicles, *J. Aircraft*, 2009, **46,** (4), pp 1340–1353.
[3] Konar, M. Redesign of morphing UAV's winglet using DS algorithm based ANFIS model, *Aircraft Eng. Aerospace Technol.*, 2019a, **91,** (9), pp 1214–1222.
[4] Konar, M. Simultaneous determination of maximum acceleration and endurance of morphing UAV with ABC algorithm-based model, *Aircraft Eng. Aerospace Technol.*, 2020, **92,** (4), pp 579–586.
[5] Ozkat, E.C., Bektas, O., Nielsen, M.J. and la Cour-Harbo, A. A data-driven predictive maintenance model to estimate RUL in a multi-rotor UAS, *Int. J. Micro Air Veh.*, 2023, **15**.
[6] Traub, L.W. Range and endurance estimates for battery-powered aircraft, *J. Aircraft*, 2011, **48,** (2), pp 703–707.
[7] Fusato, D. and Celi, R. Multidisciplinary design optimization for helicopter aeromechanics and handling qualities, *J. Aircraft*, 2006, **43,** (1), pp 241–252.
[8] Ganguli, R. Optimum design of a helicopter rotor for low vibration using aeroelastic analysis and response surface methods, *J. Sound Vibr.*, 2002, **258,** (2), pp 327–344.
[9] Grigoriadis, K.M., Carpenter, M.J., Zhu, G. and Skelton, R.E. Optimal redesign of linear systems, Proceedings of the American Control Conference, San Francisco, CA, USA, 1993, pp 2680–2684.
[10] Grigoriadis, K.M., Zhu, G. and Skelton, R.E. Optimal redesign of linear systems, *J. Dyn. Syst. Meas. Control*, 1996, **118,** (3), pp 598–605.
[11] Konar, M., Turkmen, A. and Oktay, T. Improvement of the thrust-torque ratio of an unmanned helicopter by using the ABC algorithm, *Aircraft Eng. Aerospace Technol.*, 2020, **92,** (8), pp 1133–1139.
[12] Oktay T. and Sultan C. Flight control energy saving via helicopter rotor active morphing, *J. Aircraft*, 2014, **51,** (6), pp 1784–1804.
[13] Konar, M. GAO algoritma tabanli YSA modeliyle İHA motorunun performansinin ve uçuş süresinin maksimizasyonu, *Eur. J. Sci. Technol.*, 2019b, **15**, pp 360–367.
[14] Leishman, G.J. *Principles of Helicopter Aerodynamics*, 2nd ed, Cambridge University Press, 2016.
[15] Padfield, G.D. *Helicopter Flight Dynamics: The Theory and Application of Flying Qualities and Simulation Modeling*, 2nd ed, Blackwell Publishing, 2007.
[16] Prouty, R.W. *Helicopter Performance, Stability and Control*, Robert E. Kreiger Publishing Co, 2005.

https://doi.org/10.1017/aer.2024.44 Published online by Cambridge University Press

[17] Seddon, J.M. and Newman, S. *Basic Helicopter Aerodynamics*, John Wiley & Sons, 2011.
[18] Bramwell, A.R.S., Done, G. and Balmford, D. *Bramwell's Helicopter Dynamics*, 2nd ed, Elsevier, 2001.
[19] Celi, R. *Helicopter Stability and Control*, Lecturer Notes, University of Maryland, 2005.
[20] Dreier, M.E. *Introduction to Helicopter and Tiltrotor Flight Simulation*, AIAA Education Series, 2007.
[21] Johnson, W. *Helicopter Theory*, Dover Publications, Inc, 1994.
[22] Oktay T. Constrained Control of Complex Helicopter Models, PhD thesis, Virginia Tech University, 2012.
[23] Oktay T. and Sultan C. Simultaneous helicopter and control-system design, *J. Aircraft*, 2013, **50,** (3), pp 911–925.
[24] Prouty, R.W. Helicopter Aerodynamics: Volume I, 2009, Lulu.com.
[25] Raptis, I.A. and Valavanis, K.P. *Linear and Nonlinear Control of Small-Scale Unmanned Helicopters*, Springer, 2011.
[26] Ren, B., Ge, S.S., Chen, C., Fua, C.H. and Lee, T.H. *Modeling, Control and Coordination of Helicopter Systems*, Springer, 2011.
[27] Watkinson J. *The Art of the Helicopter*, Elsevier, 2004.
[28] Civicioglu, P. Backtracking search optimization algorithm for numerical optimization problems, *Appl. Math. Comput.*, 2013, **219,** (15), pp 8121–8144.
[29] Civicioglu, P. and Besdok, E. A+ Evolutionary search algorithm and QR decomposition based rotation invariant crossover operator, *Exp. Syst. Appl.*, 2018, **103**, pp 49–62.
[30] Civicioglu, P., Besdok, E., Günen, M.A. and Atasever, Ü.H. Weighted differential evolution algorithm for numerical function optimization: a comparative study with cuckoo search, artificial bee colony, adaptive differential evolution, and backtracking search optimization algorithms, *Neural Comput. Appl.*, 2020, **32,** (8), pp 3923–3937.

Cite this article: Konar M. and Arık Hatipoğlu S. (2024). Maximisation the autonomous flight performance of unmanned helicopter using BSO algorithm. *The Aeronautical Journal*, **128**, 2656–2667. https://doi.org/10.1017/aer.2024.44

https://doi.org/10.1017/aer.2024.44 Published online by Cambridge University Press